SECED 2023 Conference
Earthquake Engineering & Dynamics for a Sustainable Future
14-15 September 2023, Cambridge, UK

CONSISTENCY EVALUATION OF GROUND MOTION PREDICTION EQUATIONS WITH STRONG MOTION RECORDS FROM DENSE URBAN NETWORK OF ISTANBUL

Fatma Sevil MALCIOGLU[1] & Erdal SAFAK[2]

Abstract: *The data sets of ground motion models commonly include strong ground motions that incorporate earthquakes in different regions of the world with different source, path, and site characteristics in order to build large databases. As a result, the local regional features may not be accurately reflected in GMPEs. The present study offers a comprehensive comparison between ground motion parameters estimated by the frequently used GMPEs in İstanbul and their observed values calculated from small-to-moderate ($4.0<M_L<5.7$) earthquakes from 2012 to 2022. The earthquakes are recorded by the Istanbul Earthquake Early Warning and Rapid Response Network, established and operated by Kandilli Observatory and Earthquake Research Institute of Bogazici University. A thorough examination has been conducted on the 6534 horizontal recordings from 78 events with a maximum epicentral distance of 200 km. Nonlinear regression analyses of actual data are carried out, using similar functional forms of the selected GMPEs. The comparison of the regression line of this study with the selected GMPEs shows the overestimation tendency of all ground motion models. Additionally, the residual analyses are performed to assess the consistency between actual and predicted parameters and support the higher estimation trend of the GMPEs. Total residuals are further split into between-event and within-event components. The predominance of negative between-event residuals may signify the implications of regional source attributes on ground motions. Negative and positive variations of within-event residuals, on the other hand, may be an indicator of regional disparities in attenuation that cannot be accounted by distance and V_{S30} variables.*

Introduction

In 1999, Istanbul was shaken by two notable earthquakes, namely the M_W7.4 Kocaeli and M_W7.2 Düzce Earthquakes, which took place on the NAFZ in the immediate east of the city and inflicted devastating structural damage and thousands of fatalities. The region will likely experience a catastrophic earthquake of a large magnitude in the near future and Istanbul remains one of the seismically riskiest cities (Le Pichon, et al., 2003). The high probability of such a large event makes the assessment of the seismic hazard, which necessitates for reliable estimates of the ground motion parameters, more and more crucial for the region. In this regard, various researchers have attempted to perform comprehensive seismic risk and hazard assessments for the region to identify the ground motion levels and their possible consequences (e.g. Şeşetyan et al.,2019).To estimate the ground motion parameter in the case of an expected event, ground motion prediction equations (GMPEs) are frequently employed as the vital element of probabilistic or deterministic seismic hazard assessment. However, in order to build large databases, the data sets of these models commonly include strong ground motions that incorporate earthquakes with different regions of the world with different source, path, and site characteristics. As a result, the local regional features may not be accurately reflected in GMPEs. The geological peculiarities in Türkiye may have a considerable impact on regional ground motion estimates, as emphasized in a recent study by Kotha et al., 2020. The study's findings demonstrate the necessity for regional ground motion models because, in contrast to the pan-European ground motion models that had previously been proposed, residual variances increase with the contribution of regional data.

Consequently, the objective of the present study is to explore the consistency between observed ground motion characteristics of small-to-moderate magnitude events that occurred near Istanbul and the extensively used GMPEs in the vicinity. First, nonlinear regression is applied to the entire database as well as groups that are classified based on their magnitude levels. To provide a quick

[1] PhD Candidate, Bogazici University, KOERI, Department of Earthquake Engineering, Istanbul, Turkiye, sevil.malcioglu@boun.edu.tr
[2] Prof. Dr., Bogazici University, KOERI, Department of Earthquake Engineering, Istanbul, Turkiye

assessment, the actual ground motion parameters and their prediction lines derived from this study are compared with selected GMPEs. Then, total residuals are computed for each GMPE selected and split into their between-event and within-event terms to provide a more comprehensive quantitative assessment of the GMPEs' efficiency.

Compilation of ground motion database

The existence of a robust strong ground motion database is the primary and most indispensable component in order to test the consistency of GMPEs with the regional ground motions. Istanbul Earthquake Rapid Response and Early Warning System (IERREWS), which has been initiated to mitigate the losses in the case of a disastrous earthquake in Istanbul by the Department of Earthquake Engineering of Boğaziçi University, Kandilli Observatory Earthquake Research Institute (KOERI) with the cooperation of the Governorate of Istanbul, First Army Headquarters and Istanbul Metropolitan Municipality, comprises a dense strong ground motion network in İstanbul (Şeşetyan et al., 2011). In addition to early warning and rapid response studies, this dense urban network also offers an extensive database for earthquake engineering studies e.g. assessment of the consistency of the GMPEs that are widely used in seismic hazard studies.

IERREWS has recorded numerous small-to-moderate magnitude ($M_L \leq 5.7$) events since 2012. We have meticulously examined the initial database by applying our database criteria. The documental problems such as repeated files, lack of component recordings, etc. in the initial raw database have been detected and the earthquakes and recordings associated with these problems have been eliminated. Since many global GMPEs' databases are limited for seismic events larger than M≥4.0 and ground motions recorded at stations closer than 200 km, we have decided to be restricted our data by the aforementioned magnitude and distance limits.

The ground motion signal in the raw data may occasionally be contaminated by undesired random noises. Ground motion processing is an essential step in decontaminating the frequency content and acquiring reliable information for earthquake engineering studies. According to Douglas and Boore, 2011, despite the high-frequency noise contamination in the ground motions, the need for low-pass filtering is not always a mandatory application. The low-pass filter frequency (f_{lp}) has been kept constant at 20 Hz for the removal of high-frequency noises. In contrast to the negligible influence of high-frequency noises, low-frequency noise interference may have a significant deceptive effect on strong ground motion parameters. That's why, high-pass corner frequencies have been identified for each component individually by examining the integrated velocity and displacement time histories. Almost 90 percent of the recordings have chosen high-pass filter frequencies below 0.3 Hz. A few cases necessitated the f_{hp} to be raised to a maximum of 0.5 Hz. The ground motion recordings have been filtered with a 4th-order band-pass Butterworth filter between the corner frequencies mentioned above. Moreover, recordings that are not still de-contaminated from noise despite the filtering process and contain interruptions within wave packages have been assigned *as "unqualified records"* and have been omitted from the database. The recordings with multiple shocks require additional data processing and in these records, the smallest shock has been systematically eliminated by picking up the largest event. Finally, it should be noticed that the majority of recordings from a smaller dataset (438 individual records from M_W 4.7 and M_W 5.7 Silivri earthquakes) are of high quality and have a wide range of usable frequency (up to ~50 Hz) (Malcioglu et al., 2022a).

After data selection criteria and the processing stage have been applied to the initial database, the final database currently comprises 6534 individual horizontal-component recordings from 78 seismic events that occurred around the Marmara region. The strike-slip mechanism seems to be dominant in the majority of the events, whose focal mechanisms are documented and the focal depth of the events varies from 2 km to 20 km. Figure 1a illustrates the spatial distribution of strong ground motion stations and earthquakes which are utilized in the final database. The database has a local magnitude (M_L) range of 4.0 to 5.7, and the epicentral distances range from 2 to 200 km with a mean of 117 km (Figure 1b).

Main characteristics of the selected GMPEs

Numerous empirical equations exist that estimate the ground motion parameters relying mostly on the tectonic regime, earthquake magnitude, source-to-site distance, soil condition, etc. The GMPEs from the compendium of Douglas, 2022 have been meticulously reviewed regarding whether events from Türkiye were included in their database and their usage frequency in the earthquake engineering studies considering İstanbul for the selection of the GMPEs in this study.

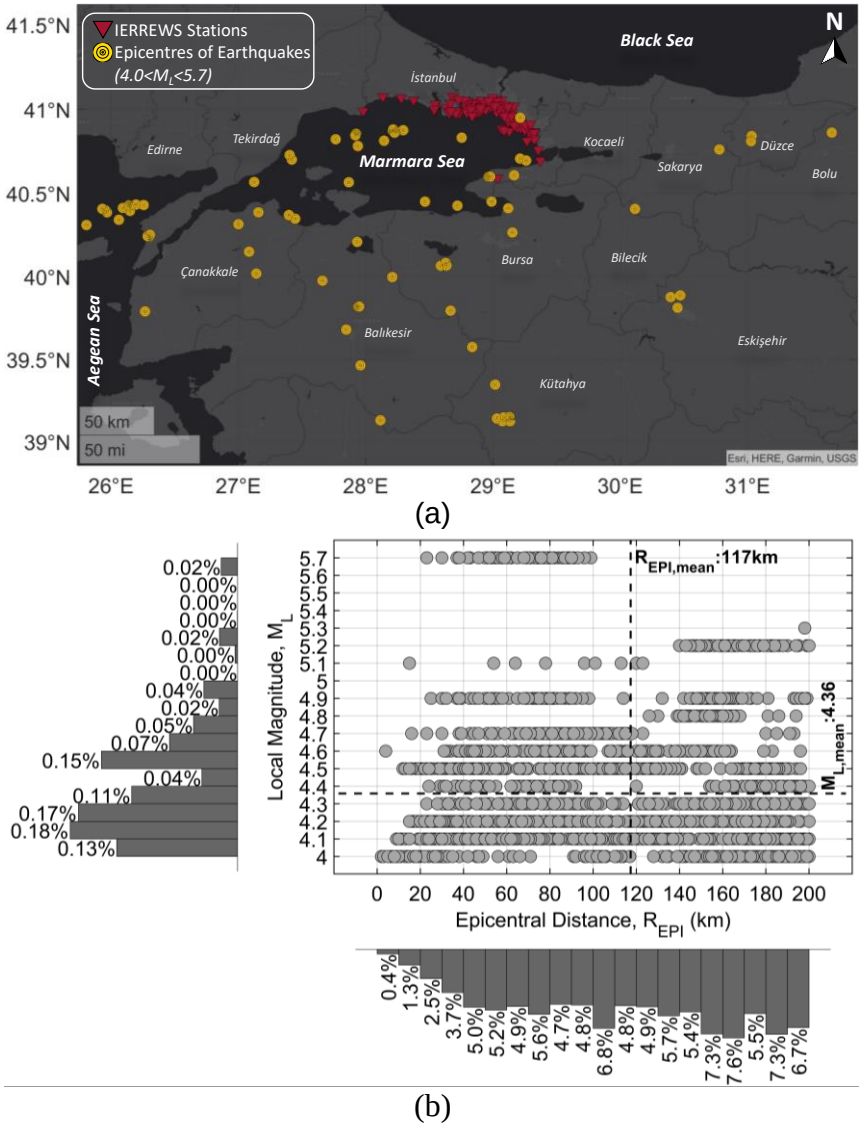

Figure 1. (a) Spatial distribution of the earthquakes' epicentres (2012-2022) and IERREWS network stations, (b) Local magnitude (M_L) and epicentral distance (R_{EPI}) distribution of the strong ground motion records (Number of data=3267) in the database.

A significant number of earthquakes from Türkiye have been identified in the two most recent GMPEs, Kuehn and Scherbaum, 2016 and Kotha et al., 2020. However, PGV and spectral accelerations, which this study took into account for the comparative evaluation, have not been incorporated into Kuehn and Scherbaum's ground motion model. Also, due to the lack of accessibility of several of the coefficients of Kotha et al., 2020, we were also unable to employ the latter in our research. Table 1 provides an overview of the selected three GMPEs' details, including their abbreviations, which will be utilized throughout this study, the type of dependent and independent variables and their ranges specified in their databases and their references. The event magnitude, distance measure, site parameter, and style-of-faulting (SoF) are the primary independent input parameters jointly utilized in the GMPEs chosen herein. The moment magnitude (M_W) rather than M_L, which is employed in our database, is considered as a magnitude scale to specify the size of earthquakes in all of the GMPEs selected in this study. However, no magnitude conversion has been applied in our database since the M_L for events at this level can be assumed to be similar to M_W (Heaton et al., 1986). In BSSA14 and KAAH15, Joyner-Boore distance (R_{JB}) serves as the only distance measure, whereas ASB14 provides ground motion models for three different distance metric types, including epicentral distance (R_{EPI}), Joyner-Boore distance (R_{JB}), and hypocentral distance (R_{HYPO}). This study considers the epicentral distance (R_{EPI}) since the fault rupture geometry of the majority of small-to-moderate events in our database

does not exist. However, it should be emphasized that the difference between R_{JB} and R_{EPI} may be considered insignificant due to the small size of fault rupture plane of low-to-moderate-sized events (M<6.0) (Ambraseys et al., 2005). Therefore, R_{JB} is regarded as being equivalent to R_{EPI} in the analyses. The V_{S30} parameter specifies the site condition for all chosen GMPEs. For Istanbul, station-based V_{S30} metrics have been deduced from V_{S30} maps of the Istanbul Metropolitan Municipality (OYO, 2007 and 2009). 80 percent of the stations fall within the V_{S30}s range of 180-760 m/s. Given its dominance in the database and as the principal faulting mechanism of the NAFZ, the style-of-faulting is presumed to be a strike-slip mechanism in the analyses. The basin depth ($Z_{1.0}$), which is the depth from the ground surface to the level of V_{S30}=1.0 km/s, is another required parameter for only the ground motion model of BSSA14. As $Z_{1.0}$ values are not supplied at the recording sites, this parameter has been separately calculated via V_{S30}-based empirical equations recommended by Kaklamanos et al., 2011. Also, as opposed to ASB14, BSSA14 and KAAH15 allow users to choose a specific region, which includes Türkiye. The ASB14, on the other hand, can be employed directly without any regional adjustment because its database consists of strong ground motions gathered in the Middle East and the Mediterranean region.

Abbreviation	Magnitude Type Range	Distance Type Range	Ground Motion Parameter*	Site Parameter	Style of Faulting**	Reference
ASB14	M_W 4.0-7.6	R_{JB} R_{HYPO} R_{EPI} ≤ 200 km	PGA PGV, SA (T=0.01-4.0 s)	V_{S30}	NF SSF RF	Akkar et al., 2014
BSSA14	M_W 3.0-7.9	R_{JB} ≤ 400 km	PGA PGV, SA (T=0.01-10.0 s)	V_{S30}	Unknown NF SSF RF	Boore et al. 2014
KAAH15	M_W 4.0-8.0	R_{JB} ≤ 200 km	PGA PGV, SA (T=0.01-4.0 s)	V_{S30}	NF SSF RF	Kale et al., 2015

Table 1. Main features of the selected GMPEs
*(*PGA: Peak ground acceleration; PGV: Peak ground velocity; SA: Spectral accelerations at the periods (T), **NF: Normal fault, SSF: Strike slip fault; RF: Reverse fault)*

Consistency Evaluation Methods and Results

Comparison of attenuations with distance

The attenuation of the actual ground motion parameters with distance is initially compared to the selected ground motion models (ASB14, BSSA14 and KAAH15). Additionally, a two-stage nonlinear least square regression analysis is performed on the entire database (M_L≤5.7) as well as on sub-datasets that are categorized depending on their magnitude levels to provide a general comparison with GMPEs. It should be stated that the main intention of the nonlinear regressions in this study is not to generate a new GMPE for the region. They are merely produced in order to simplify the interpretation of the comparison. The functional forms of source and path terms are taken as similar to ASB14, which provides regression coefficients considering the epicentral distances. The general functional form used in the nonlinear regression analysis is given in Equations (1) and (2).

$$\ln(GMP) = \boldsymbol{a}_1 + \boldsymbol{a}_2(\boldsymbol{M}_L - 6.75) + \boldsymbol{a}_3(8.5 - \boldsymbol{M}_L)^2 + \left[\boldsymbol{a}_4 + \boldsymbol{a}_5(\boldsymbol{M}_L - 6.75)\right]\boldsymbol{ln}\left(\sqrt{\boldsymbol{R}_{EPI}^2 + \boldsymbol{a}_6^2}\right) \quad (1)$$

in which

$$\boldsymbol{a}_1 = \boldsymbol{b}_1 + b_2\boldsymbol{ln}(V_{\boldsymbol{S30}}) \quad (2)$$

Where, GMP refers to the dependent variable of the equation and herein geometric mean of the interested ground motion parameter such as PGA, PGV or SA. a_1, a_2, a_3, a_4, a_5 a_6,a_7, b_1 and b_2 are coefficients computed via regression analysis whereas M_L, R_{EPI} and V_{S30} refer to local

magnitude, epicentral distance and average shear wave velocity for the upper 30 m depth. The numeric values in the functional form are taken similarly to those in ASB14 and they are not calculated as part of regression analysis e.g. 6.75 representing the hinging magnitude. Initially, the coefficients of the source and path terms are calculated via regression through Equation (1). The coefficients b_1 and b_2 of soil condition term are then computed by executing second-stage regression between a_1, which is acquired as a result of 1st stage of the analysis, and soil condition parameters, V_{S30}. The final regression coefficients for six ground motion parameters (PGA, PGV, SA (T=0.4; 0.6; 1.0; 2.0, $\xi = 5\%$)) are provided in Table 2 for regressions executed through the entire database. It should be noted that ground motions, which are used in the calculation of spectral accelerations, are applied an elimination based on selected high-pass filter frequency in the data processing stage.

Ground Motion Parameter	b_1	a_2	a_3	a_4	a_5	a_6	b_2
PGA	14.2428	3.4262	0.1849	-1.4793	0.0173	6.1446	-0.5059
PGV	10.7527	3.7097	0.2817	-0.7863	0.1957	4.8556	-0.8091
SA (T=0.4 s)	16.5390	4.1206	0.2395	-1.1216	0.0253	8.4275	-0.9698
SA (T=0.6 s)	13.4576	3.7392	0.3219	-0.2891	0.2917	7.6062	-1.0900
SA (T=1.0 s)	12.7222	3.9846	0.3681	-0.0386	0.3633	8.5129	-1.2125
SA (T=2.0 s)	13.0681	6.0296	0.4721	-0.5750	0.1042	4.2357	-1.0594

Table 2.Total-database regression coefficients.

Ground motion parameters (PGA, PGV and SA (T=0.4; 0.6; 1.0; 2.0)) are calculated by incorporating the average V_{S30} value ($V_{S30,average}$=527 m/s) of the stations in the selected GMPEs and equations, which are derived in this study. Figure 2 shows some examples of the comparison of recorded ground motion parameters with the median lines of the selected GMPEs and the total & magnitude-based regression lines of this study. Only four magnitude levels (M_L4.2, M_L4.5, M_L4.7 and M_L4.9) of comparison figures are provided for purposes of illustration due to the page limitation. The comparative figures include both ground motion models of ASB14 generated based on R_{EPI} and R_{JB} in addition to BSSA14 and KAAH15. Due to a paucity of data throughout the whole distance range, the magnitude-based relation of this study may not be very robust for each magnitude level. Total-based regression lines appear to be consistent with the observed data; nonetheless, this is an expected trend given that the equation's database of this study has been formed by ground motion parameters provided herein. Furthermore, there seem to be numerous data points both above and below the estimations of total-based regression. This large variation around the regression line may also imply that ground motion parameters might not be represented by a single line. Even so, these regression lines, which are derived in this study, facilitate the comparison of the inclination of observed data with GMPEs. The plots point out the overestimation tendency of the selected GMPEs for all parameters. Median lines of all GMPEs result in larger values than observed ground motion parameters except for several data points. As stated previously, it is assumed that local magnitude is equivalent to moment magnitude for estimating ground motion parameters with GMPEs. However, M_W may be somewhat greater than the M_L for earthquakes from Türkiye, according to Kadirioğlu and Kartal (2016). It is essential to note that in this case, GMPEs provide larger ground motion parameters and are situated far from the lines generated by the study.The fact that the median estimates of ASB14 based on both the R_{EPI} and the R_{JB} are quite close to each other may be an indication of implementing the R_{EPI} will not result in any contradictions in the study. BSSA14 provides the highest estimations among all selected GMPEs at particularly longer epicentral distances while the highest predictions in the closest distances appear to be generally produced by ASB14. Although KAAH15 slightly yields the closest estimates to the actual data, the attenuation plots with distance in Figure 2 clearly display its overestimation tendency.

Residual Analysis

The variation of misfit between estimated and actual ground motion parameters may be tested through conventional residual analysis, which is a comparison technique in the natural logarithm domain. The underestimation of selected GMPE is signified by positive residuals whilst negative residuals imply the overestimation tendency of the GMPEs. The total residual ($\delta_{GMP,es}$) is defined

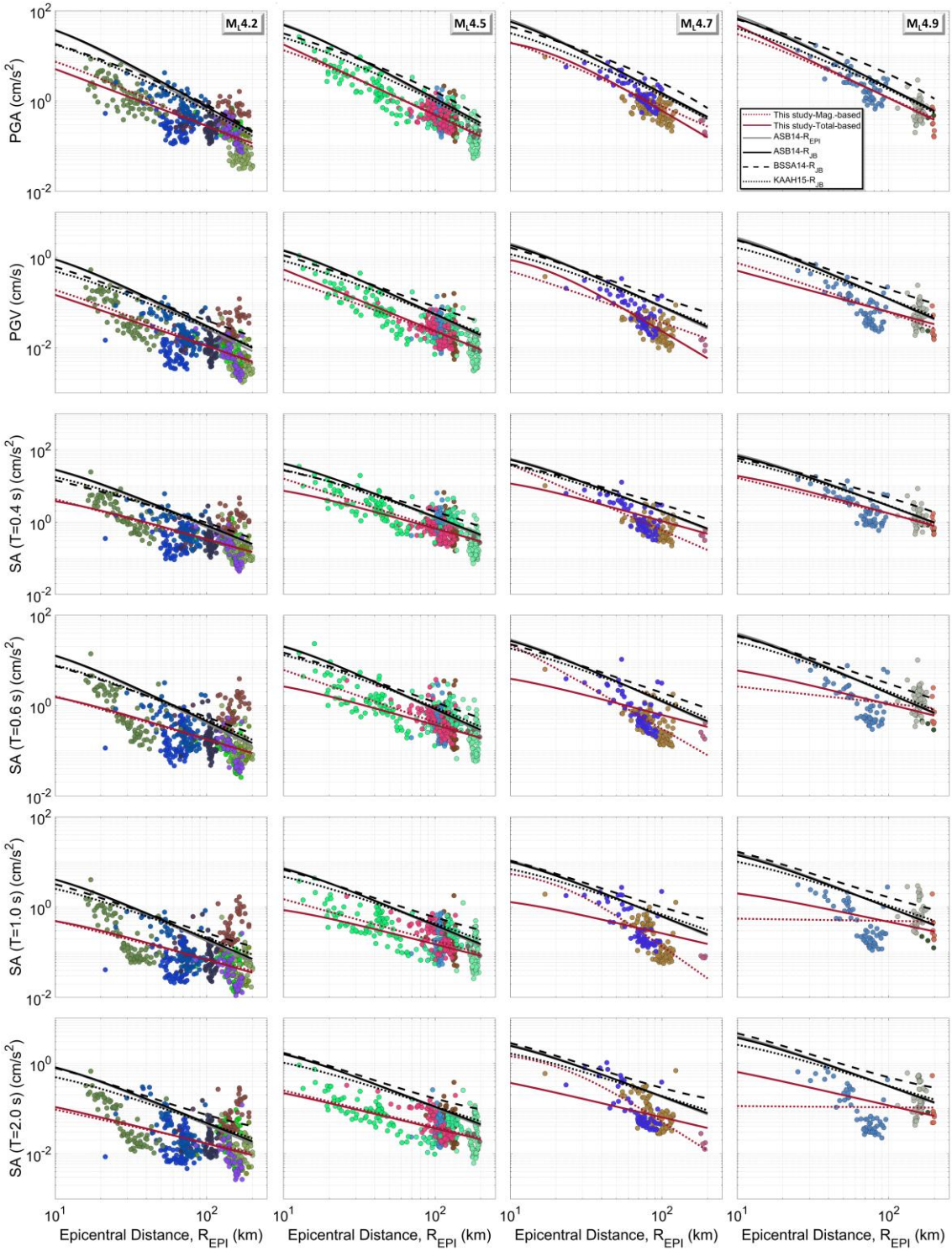

Figure 2. Comparison of recorded ground motion parameters (PGA, PGV, SA (T=0.4; 0.6; 1.0; 2.0) with median lines of the selected GMPEs ($ASB14_{R_{EPI}\text{-based}}$, $ASB14_{R_{JB}\text{-based}}$, BSSA14, KAAH15) and the total & magnitude-based regression lines of this study (Different colours of the markers refer to different events and V_{S30} value has been taken as 527 m/s in the calculation of estimation lines).

as the difference between the natural logarithm of the actual and estimated ground motion parameter (GMP) as seen in Equation (3).

$$\delta_{GMP,es} = \ln\left(GMP_{actual,es}\right) - ln\left(GMP_{estimated,es}\right) = \delta B_{GMP,e} + \delta W_{GMP,es} \quad (3)$$

In which, the variables simply allude to values at the s[th] station of the e[th] event. $GMP_{actual,ies}$ and $GMP_{estimated,es}$ are the actual and estimated median ground motion parameters, respectively. Total residuals, $\delta_{GMP,es}$ can be decomposed into components that reflect the earthquake's source, path, and site implications, e.g. between-event ($\delta B_{GMP,e}$) and within-event ($\delta W_{GMP,es}$) terms. $\delta B_{GMP,e}$ may be calculated with a least-square approach (Baltay et al., 2017), which is described by the mean difference between the actual ground motion parameters and the corresponding estimation of the ground motion model for each event (Equation (4)). The contribution of components such as stress drop and slip variation, and others, can be captured by between-event residuals (Al-Atik et al., 2010).

$$\delta B_{GMP,e} = \frac{\sum_{s=1}^{N_{st}} \ln\left(GMP_{actual,es}\right) - ln\left(GMP_{estimated,es}\right)}{N_{st}} \quad (4)$$

The variations induced by azimuthal effects, heterogeneity of the crust, deep geology, near-surface layering, etc. are represented by the within-event residuals, which are computed by the difference between the actual ground motion parameter and its median estimation corrected by the between-event term for each individual event as formulated in Equation (5) (Al-Atik et al., 2010).

$$\delta W_{GMP,es} = \ln\left(GMP_{actual,es}\right) - \left[ln\left(GMP_{estimated,es}\right) + \delta B_{GMP,e} \right] \quad (5)$$

Total, between-event and within-event residuals have been computed for the median estimations of all selected GMPEs for PGAs, PGVs and SAs (T=0.4; 0.6; 1.0; 2.0). It should be noted that each station's V_{S30} value has been considered rather than an average value of V_{S30} in the residual analyses. The result of residual analyses of PGA, PGV and SAs(T=0.4) are only reported as an example herein.

Total residuals, which are plotted against $R_{EPI,}$ are given in Figure 3. Also, the 16[th] (-σ), 50[th] (mean) and 84[th] (+σ) percentile of the normal distribution for each distance bin with 10 km of the interval are seen by the black squares and lines in the plots. The dominancy of negative total residuals for three ground motion parameters verifies the overestimation tendency of all selected GMPEs which has been detected in the preceding section. Slightly higher negative residuals and the fluctuation is noticeable particularly at distances closer than 80 km. Also, KAAH15 appears to provide the relatively lowest residuals of four GMPEs tested mainly at the entire distance range while BSSA14 is the ground motion model with the largest overestimation capacity of this regional data.

The results of between-event residuals, which reflect the source-related variability, and the mean values of bins with a magnitude interval of 0.1 with corresponding standard deviations are also plotted against M_L in Figure 4. The systematic negative between-event residuals imply that all ground motion parameters are over-predicted by the three GMPEs under consideration. Due to one each outlier event with higher between-event residuals in specifically M_L4.0 and 4.8 subgroups, their standard deviations result in exceptionally high. The standard deviations of magnitude bins after M_L4.9 could not be determined because each bin group only contains one event. Also, the fluctuations in between-event residuals seem to be more prominent below M_L4.5.

The significant negative (over-prediction) and positive (under-prediction) changes in within-event residuals, which are mostly associated with the variability due to path and site, are visible. Despite these considerable fluctuations of individual data around the zero line, the systematic variation pattern with epicentral distance cannot be identified. However, the mean of each distance bin with 10 km of interval indicates a remarkable consistency with the actual ground motion parameters along the entire distance range. Nevertheless, the within-event residuals vary in large positive and negative residuals ranging from about -2.0 to 2.0 even in each specific distance level (Figure 5a). This may not be explained via the only effect of soil conditions since the variation of within-

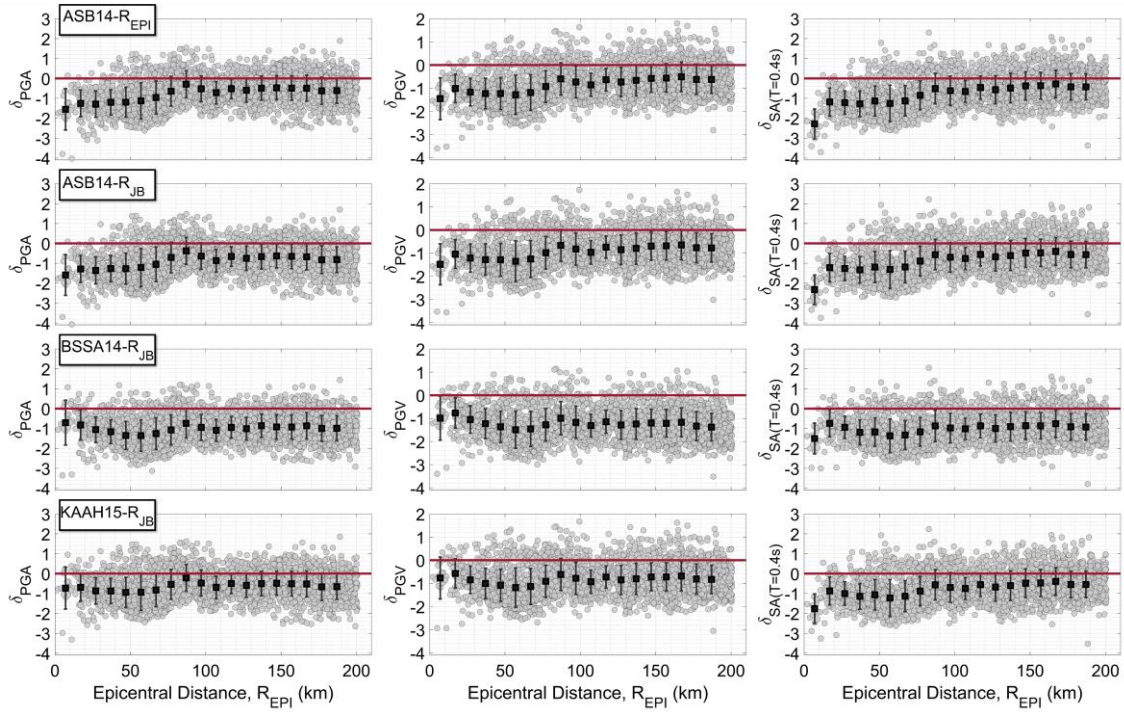

Figure 3. Variation of the total residual of PGA, PGV and SA(T=0.4 s) with epicentral distance for the selected GMPEs ($ASB14_{R_{EPI}\text{-based}}$, $ASB14_{R_{JB}\text{-based}}$, BSSA14, KAAH15) (Red lines correspond to zero level of residuals. Black squares and lines display the mean of each group with 16th and 84th percentile away from the mean).

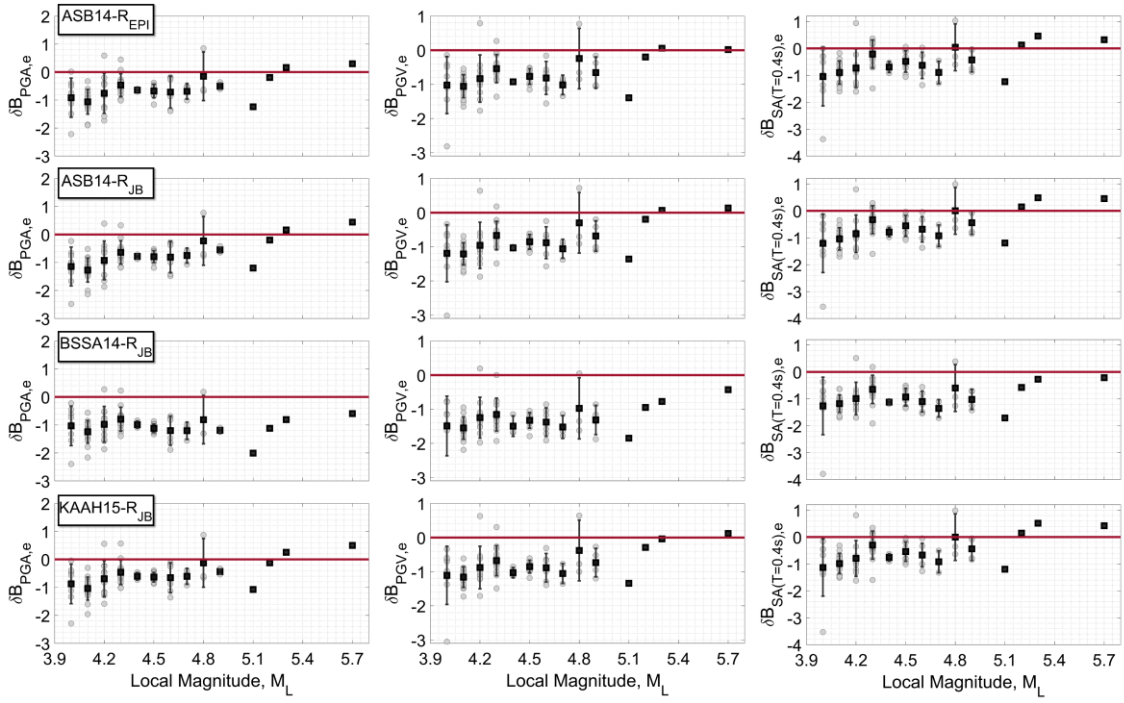

Figure 4. Variation of the between-event residual of PGA, PGV and SA (T=0.4 s) with epicentral distance for the selected GMPEs ($ASB14_{R_{EPI}\text{-based}}$, $ASB14_{R_{JB}\text{-based}}$, BSSA14, KAAH15) (Red lines correspond to zero level of residuals. Black squares and lines display the mean of each group with 16th and 84th percentile away from the mean).

event residuals with V_{S30} does not give explicit statistical implications (Figure 5b). In this context, this large variation in within-event residuals may be an indication of the other regional differences, which cannot be represented by only distance metric and V_{S30}.

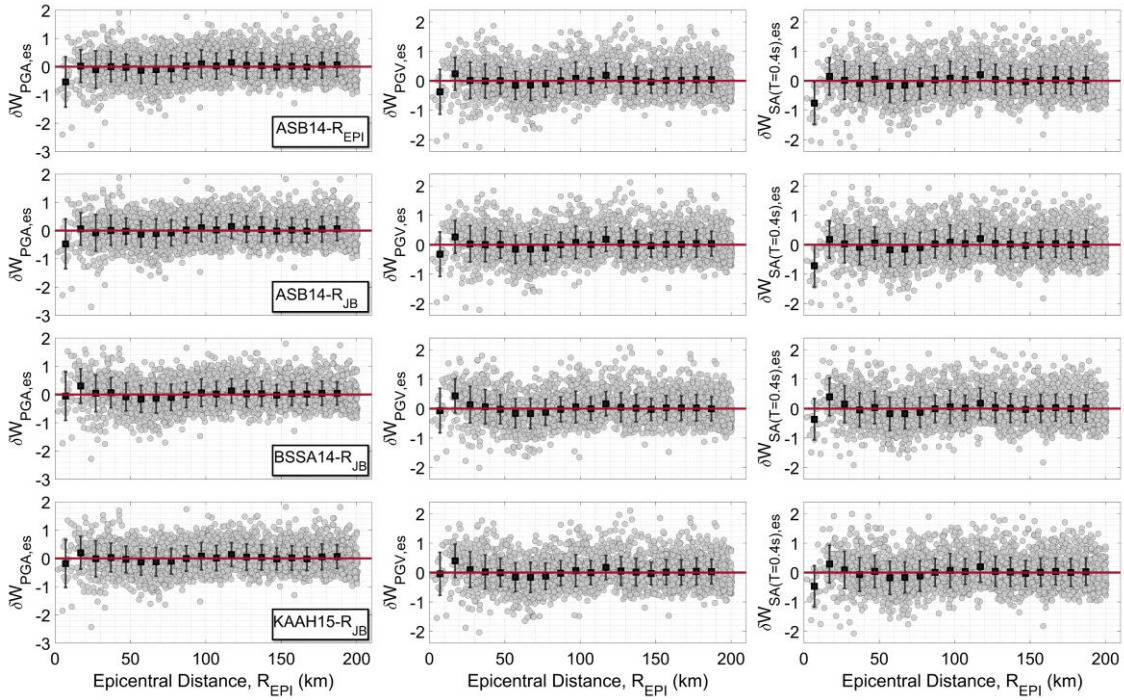

(a)

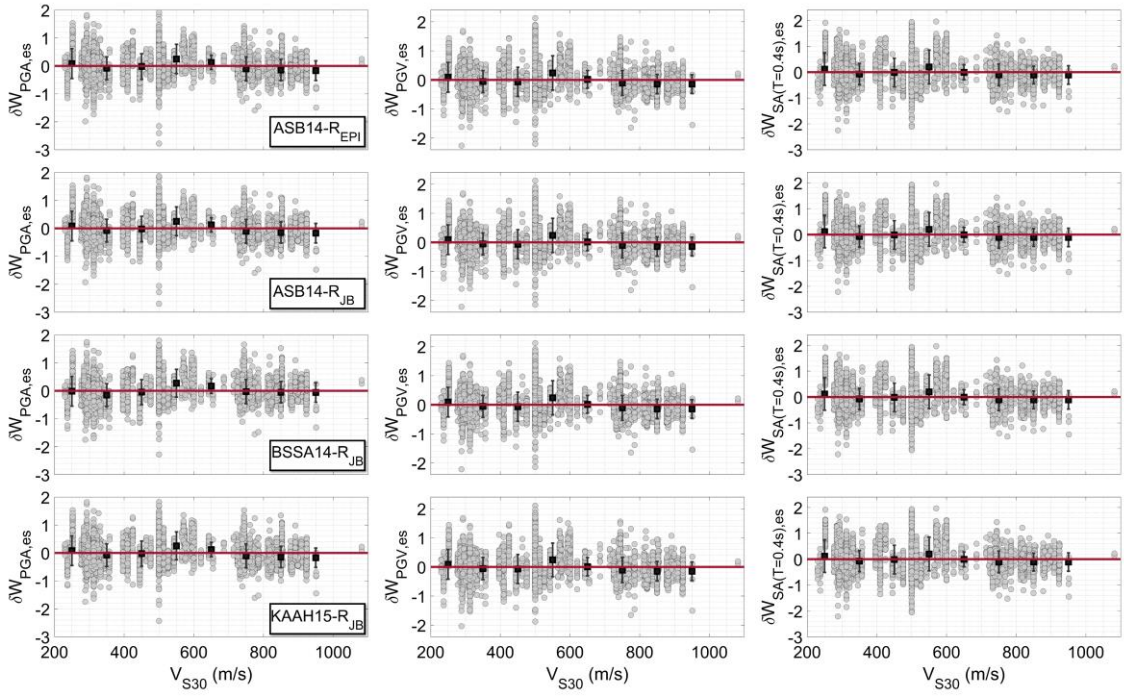

(b)

Figure 5. Variation of within-event residuals of PGA, PGV and SA(T=0.4 s) with (a) epicentral distance (b) V_{S30} for the selected GMPEs (ASB14$_{R_{EPI}\text{-based}}$, ASB14$_{R_{JB}\text{-based}}$, BSSA14, KAAH15) (Red lines correspond to zero level of residuals. Black squares and lines display the mean of each group with 16th and 84th percentile away from the mean).

Conclusion

Istanbul's dense urban network yields a plethora of small-to-moderate magnitude events, providing a perfect opportunity to evaluate the efficiency of GMPEs, which are frequently utilized in the regional seismic hazard and risk assessments of İstanbul. The functionality of three GMPEs is assessed against actual ground motion parameters of these events recorded at IERREWS stations in this study. The consistency evaluation of the GMPEs is implemented via both comparisons through attenuation of ground motion parameters with distance and the residual analysis. As the standard deviation of GMPEs is not considered by the residual analysis, alternative statistical and probabilistic methods that have been recommended in the literature may be used to evaluate the effectiveness of ground motion models and rank the GMPEs. Nevertheless, the findings acquired here clearly demonstrate that GMPEs do not adequately represent the real ground motions recorded by the IERREWS network from small- to moderate-sized events that occurred around İstanbul. The variation of both the ground motion parameters and the estimations of the equation acquired from our database in this study demonstrates that the selected GMPEs yield larger values than the actual ones. Total residuals also corroborate this outcome. The examination of between-event residuals also reveals that the GMPEs overestimate, most likely because of variations in the source characteristics of local earthquakes such as differences in stress drops of local events etc. The variation of the within-event residuals neither with epicentral distance nor with V_{S30} as a soil condition parameter does not point out any visible trend. The within-event residuals that induce both overestimation and underestimation, on the other hand, vary in a wide range. The regional features that cannot be represented by distance metrics and V_{S30} could explain variability in within-event residuals. To end, the mismatch between GMPEs and actual data may be caused by differences in attenuation characteristics imposed by regional implications such as azimuthal variations, which has to be probed at deeper level in ongoing studies. That's why, future research should also consider regional impacts to estimate ground motion parameters.

References

Ambraseys, NN, Douglas J, Sarma SK, and Smit PM (2005), Equations for estimation of strong ground motions from shallow crustal earthquakes using data from Europe and the Middle East: Horizontal peak ground acceleration and spectral acceleration, *Bulletin of Earthquake Engineering*, 3: 1–53, https://doi.org/10.1007/s10518-005-0183-0

Akkar S, Sandıkkaya MA, Bommer JJ (2014), Empirical ground-motion models for point- and extended-source crustal earthquake scenarios in Europe and the Middle East, *Bulletin of Earthquake Engineering*, 12: 359-387, https://doi.org/10.1007/s10518-013-9461-4

Al Atik L, Abrahamson N, Bommer JJ, Scherbaum F, Cotton F, Kuehn N (2010), The variability of ground motion prediction models and its components, *Seismological Research Letters*, 81(5):794-801, https://doi.org/10.1785/gssrl.81.5.794

Baltay AS, Hanks TC, Abrahamson NA (2017), Uncertainty, Variability, and Earthquake Physics in Ground - Motion Prediction Equations*, Bulletin of the Seismological Society of America* 107 (4): 1754–1772, https://doi.org/10.1785/0120160164

Boore DM, Stewart JP, Seyhan E, Atkinson GM (2014), NGA-West2 Equations for Predicting PGA, PGV, and 5% Damped PSA for Shallow Crustal Earthquakes, *Earthquake Spectra*, 30 (3):1057-1085, https://doi.org/10.1193/070113EQS184M

Douglas J (2022), *Ground motion prediction equations 1964 – 2021*, Department of Civil and Environmental Engineering, University of Strathclyde, United Kingdom, 31th May 2022

Douglas J and Boore DM (2010) High-frequency filtering of strong-motion records, *Bulletin of Earthquake Engineering*, 9, 395–409, https://doi.org/10.1007/s10518-010-9208-4

Heaton TH, Tajima F and Mori AW, (1986), Estimating ground motions using recorded accelerograms. *Surveys in Geophysics,* 8, 25–83,https://doi.org/10.1007/BF01904051

Kale Ö, Akkar S, Ansari A and Hamzehloo H (2015), A Ground - Motion Predictive Model for Iran and Turkey for Horizontal PGA, PGV, and 5% Damped Response Spectrum: Investigation of Possible Regional Effects, *Bulletin of the Seismological Society of America*, 105 (2A): 963–980, https://doi.org/10.1785/0120140134

Kadirioğlu FT and Kartal RF, (2016), The new empirical magnitude conversion relations using an improved earthquake catalogue for Turkey and its near vicinity (1900-2012), Turkish Journal of Earth Sciences, 25(4): 300-310, https://doi.org/10.3906/yer-1511-7

Kaklamanos J, Baise LG, Boore DM (2011) Estimating unknown input parameters when implementing the NGA ground-motion prediction equations in engineering practice, *Earthquake Spectra*, 27(4):1219, https://doi.org/10.1193/1.3650372

Kotha SR, Weatherill G, Bindi D, Cotton F (2020) A regionally-adaptable ground-motion model for shallow crustal earthquakes in Europe, *Bulletin of Earthquake Engineering*, 18:4091-4125, https://doi.org/10.1007/s10518-020-00869-1

Kuehn NM and Scherbaum F (2016) A partially non-ergodic ground-motion prediction equation for Europe and the Middle East, *Bulletin of Earthquake Engineering*, 14(10):2629-2642, https://doi.org/10.1007/s10518-016-9911-x

Malcioglu FS, Süleyman H and Çaktı E, (2022), Seismological and engineering characteristics of strong motion data from 24 and 26 September 2019 Marmara Sea earthquakes*, Bulletin of Earthquake Engineering*, 20, 5567–5599, https://doi.org/10.1007/s10518-022-01422-y

Le Pichon X, Chamot-Rooke N, and Rangin C (2003), The North Anatolian Fault in the Sea of Marmara, *Journal of Geophysical Research*, 108(B4): 2179, https://doi.org/10.1029/2002JB001862

OYO Inc., Japan, 2007. *Production of Microzonation report and maps on European side (south)*. Final report to Istanbul Metropolitan Municipality

OYO Inc., Japan, 2009. *Production of microzonation report and maps on Asian side*, Final report to Istanbul Metropolitan Municipality

Şeşetyan K, Demircioğlu Tümsa, M and Akinci A (2019), Evaluation of The Seismic Hazard in The Marmara Region (Turkey) Based on Updated Databases, *Geosciences*, 9(12): 489-524, https://doi.org/10.3390/geosciences9120489

Şeşetyan K, Zülfikar C, Demircioğlu M, Hancılar U, Kamer Y and Erdik M (2011), Istanbul Earthquake Rapid Response System: Methods and practices, *Soil Dynamics and Earthquake Engineering*, 31(2011): 170-180, https://doi.org/10.1016/j.soildyn.2010.02.012